Journal of Analysis and Testing
https://doi.org/10.1007/s41664-020-00139-8

ORIGINAL PAPER

Targeted Metabolomics Revealed the Regulatory Role of Manganese on Small-Molecule Metabolism of Biofilm Formation in *Escherichia coli*

Rui Guo[1,2] · **Haitao Lu**[1,2]

Received: 23 April 2020 / Accepted: 1 June 2020

Abstract
Biofilms are special microbial communities produced by many microorganisms, such as bacteria, viruses, and fungi. Biofilms enable the microorganisms to possess the capacity against a diversity of stressful environments. Yet, biofilm formation often causes tough challenges in clinical infections, food quality, and environmental issues, however, the formation mechanism of biofilms are still incompletely understood which seriously impedes the development of new strategies to eradicate biofilms in different niches. In this study, we sought to explore the regulatory role of manganese (Mn^{2+}) on small-molecule metabolism of biofilm formation in *Escherichia coli* (*E. coli*). Using structural imaging assay combined with precision-targeted metabolomics method, to investigate how biofilm formation responded to various concentrations of Mn^{2+}, we found that Mn^{2+} could inhibit biofilm formation through the regulation of phenotypic morphology and metabolic reprogramming. Collectively, our work discovered 16 differential functional metabolites and associated three metabolic pathways involving glycolysis, TCA cycle, and tryptophan metabolism that were changed mostly by Mn^{2+} during biofilm formation, which can differentiate biofilms from the relevant planktonic cells. Altogether, this study demonstrated that Mn^{2+} can inhibit biofilm formation to regulate metabolic reprogramming and micro-structure, such effort provides novel insight into the regulation of metabolic features of biofilm formation, which enables the development of new strategies to eradicate biofilm formation for addressing the challenging problems in different areas by targeting the regulation of Mn^{2+} to the biosynthesis and expressions of functional metabolites produced by different microorganisms.

Keywords Biofilms · Manganese · Precision-targeted metabolomics · Imaging assay · Small-molecule metabolism · *Escherichia coli*

1 Introduction

Biofilms are special microbial communities that are produced by a diversity of microorganisms, such as bacteria, fungi, and viruses [1]. Microorganism related biofilms often exert high-resistance to the stressful environments due to the self-produced unique matrix containing components of nucleotides, proteins, and extracellular polysaccharides [2–4]. Basically, the biochemical process of biofilm formation involves reversible attachment, microcolony formation, and biofilm maturation. When the adhesion becomes irreversible, microbial cells shall trigger biofilm formation. However, biofilm formation often causes harmful impacts in different fields, while biofilms can decrease food quality, cause environmental pollution, and even can lead to high-frequency antibiotic resistance and infectious recurrence in clinic [4–6]. Unfortunately, biochemical characteristics of biofilm formation remain incompletely understood, even though the scientific community has made great efforts on the exploration of biofilm formation over past decades. Prior to this investigation, we have found that biofilm formation can cause greatly metabolic reprogramming as biofilms have a unique metabolic pattern compared to their planktonic community [7, 8]. Therefore, capturing differential

Electronic supplementary material The online version of this article (https://doi.org/10.1007/s41664-020-00139-8) contains supplementary material, which is available to authorized users.

✉ Haitao Lu
haitao.lu@sjtu.edu.cn

[1] Key Laboratory of Systems Biomedicine (Ministry of Education), Shanghai Center for Systems Biomedicine, Shanghai Jiao Tong University, Shanghai 200240, China

[2] Laboratory for Functional Metabolomics Science, Shanghai Jiao Tong University, Shanghai 200240, China

Published online: 08 June 2020

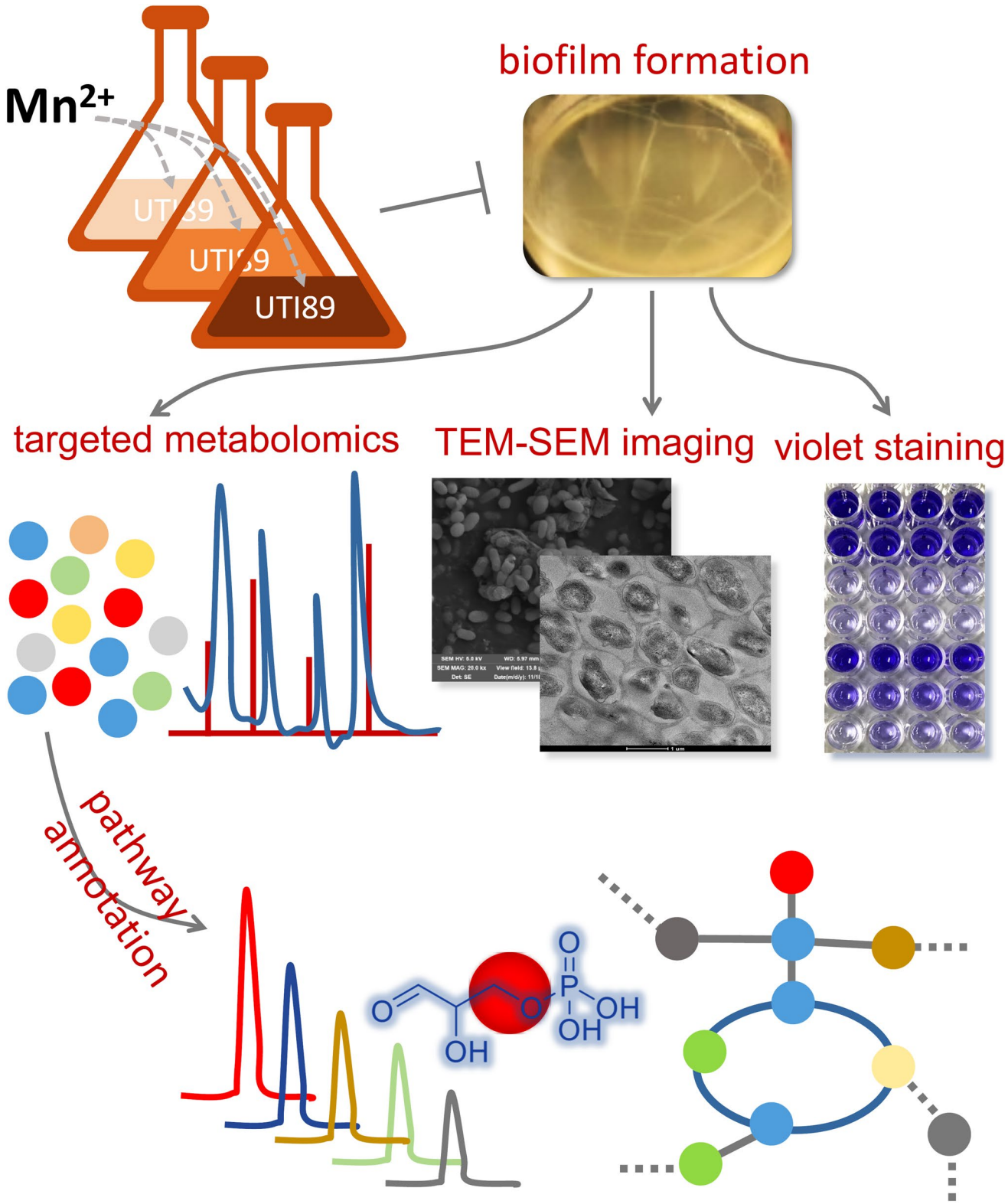

metabolism is supposed to be a new strategy to further explore the formation mechanism of biofilms.

In addition, many metals are vital for the survival of microorganisms, because they are necessary for different biological processes, including DNA replication, transcription, and respiration, etc.[9]. Metals also play an important role in biofilm formation with different microorganisms [10–12], while some studies have demonstrated

◂**Fig. 1** The study-workflow illustration to decipher the metabolic impact of Mn^{2+} on biofilm formation in *E. coli*. We combined precision-targeted metabolomics, SEM-TEM imaging, and violet staining assay to phenotype the regulatory role of Mn^{2+} during biofilm formation. Changing the concentration of Mn^{2+} in culture medium, firstly, we observed the structural changes that responded to Mn^{2+} treatment, by which we can visualize the direct impact of Mn^{2+} on biofilm formation; Secondly, violet assay also directly phenotype such role of Mn^{2+}. Thirdly, we collected metabolomics data to identify unique metabolites and associated metabolic pathways whose modifications and modulations can demonstrate metabolic impact of Mn^{2+}, which pertain the capacity to design and develop new strategy for biofilm clearance in different niches from metabolic perspective

that Mn^{2+} can regulate biofilm formation produced by several organisms such as *Bacillus subtilis*, *Streptococcus mutans* and *Candida parapsilosis* [9, 13, 14].

In the present study, we utilized *Escherichia coli* (*E. coli*) (UPEC) UTI89 as an organism-model, to investigate the metabolic impact of Mn^{2+} on biofilm formation, which could form stable biofilms during the infections, to induce high recurrence and antibiotic resistance [15–18]. When we increased the concentrations of Mn^{2+} in the culture medium, biofilm formation was influenced remarkably, the biochemical structure of biofilms was also significantly modified by Mn^{2+} that gradually tends to the phenotype of freely planktonic cells. In addition, we were the first to characterize small-molecule metabolism of biofilms which was markedly regulated by Mn^{2+}, while glycolysis, tricarboxylic acid (TCA) cycle, and tryptophan metabolism were significantly altered. Collectively, our findings shall provide novel insight into the metabolic pattern of biofilm formation under the regulation of Mn^{2+}, thus, we can design and develop new strategies to eradicate biofilms by the regulation of Mn^{2+} to biosynthesis and expressions of key functional metabolite produced by microorganisms. The study-workflow is shown in Fig. 1.

2 Materials and Methods

2.1 Chemicals and Reagents

HPLC-grade acetonitrile, methanol and formic acid were purchased from Fisher Scientific Co., Ltd (Shanghai, China). LB broth (Luria – Bertani) and LB agar were purchased from Becton Dickinson (Franklin Lakes, USA). Distilled water was purchased from Watsons Co., Ltd (Guangzhou, China). Casamino acid, yeast extract, magnesium sulfate, and manganese chloride were purchased from Sigma-Aldrich Co., Ltd (USA) and they are all of the analytical grade.

2.2 Bacterial Strains and Cell Culture

After 12 h LB-agar plate cultivation, one colony of the UTI89 strain was further incubated in LB broth for 4 h, then the solution was diluted at a ratio of 1:1000 into colony-forming antigen (CFA) medium (1% casamino acids, 0.15% yeast extract, 0.005% magnesium sulfate, and 0.0005% manganese chloride) and incubated for another 72 h at 30 °C to trigger mature biofilm formation. For the preparation of culture medium treated with different concentrations of $MnCl_2$, the analytical compound of $MnCl_2$ was added to the CFA medium at the defined different concentrations, and the left procedures were kept the same as the protocol listed above.

2.3 Sample Preparation for Targeted Metabolomics Analysis

After 72 h of culture, the planktonic cells were isolated from the solutions, and the biofilms were washed with 2 mL of PBS solvent for three times. Then, both planktonic cells and biofilm solutions were centrifuged at 2000 rpm under 4 °C for 15 min to collect the pellets. All the pellets were dissolved into 2 mL of 80% ice-cold methanol, and the mixed solution was homogenized on ice for 2 min (repeated for three times). Next, the samples were centrifuged at 12,000 rpm at 4 °C for 15 min to collect the supernatants. The supernatants were further mixed with 800 µL of ice-cold acetonitrile for 20 min before proceeding to the centrifugation at 12,000 rpm under 4 °C for 15 min. At last, the supernatants were gone through a 0.22 µm filter membrane (nylon) before lyophilization. The lyophilized samples were stored at − 80 °C until metabolomics analysis.

2.4 Targeted Metabolomics Method

Precision-targeted metabolomics analysis can refer to our newly developed precision-targeted metabolomics method [19–21]. The lyophilized samples were resuspended in 200 µL of distilled water, and then all the samples were placed on a UHPLC sample-tray at 10 °C with a 5 µL-volume injection for targeted-metabolomics analysis, which was performed on an UHPLC-QQQ/MS system (Agilent 6495 QQQ, Agilent Technologies, USA; Agilent 1290 Infinity, Agilent Technologies, USA) equipped with an ESI source with Agilent Jet Steam Technology in both negative and positive ion-modes, with a capillary voltage of 4000 V in positive mode and 3500 V in negative mode; sheath and dry gas temperature were set at 380 °C and 250 °C, respectively; sheath and dry gas flow rate were set at 12 and 16 L/min, respectively; nozzle voltage and nebulizer pressure were set at 1500 V and 20 psi, respectively. UHPLC separation of analytical samples was carried out on a Waters ACQUITY UPLC HSS T3 column (2.1 × 100 mm, 1.8 µm)

with an optimized gradient-elution program as follows: 0–2 min, 98% A; 2–10 min, 98–65% A; 10–12 min, 65–20% A; 12–14 min, 20–2% A; 14–30 min, 2% A; mobile phase A and B were 0.1% formic acid in water and acetonitrile (*V/V*), respectively. The flow rate was set at 0.3 mL/min, and the column temperature was kept at 40 °C, while the acquisition time was set at 14 min. The dynamic MRM parameters for targeted metabolomics analysis involving 240 metabolites have been recorded in our preprint publication [19], our investigation covered 143 metabolites of interest with quality metabolite peak-shape and sensitivity (Table S1).

2.5 CFU Measurement

Biofilms were dispersed in cold PBS with manual-homogenizer for 10 times with the same physical pressure to collect the free bacterial cells. The biofilm suspensions and planktonic cells were used to measure the CFU value. The following steps were recorded in a previous publication [20].

2.6 Crystal Violet Staining Assay

Biofilm formation was quantified by crystal violet staining assay. Briefly, the mature biofilm was washed three times with PBS, and then to fix the biofilm by methanol for 15 min. After the methanol was vaporized, 100 µL of 0.01% crystal violet was put into the biofilm and incubated at room temperature for 20 min. The dye wells with crystal violet were washed for five times with PBS. Bound crystal violet was solubilized with 100 µL of 30% acetic acid for 30 min and then shaken slowly. The OD was measured with a microplate reader at the wavelength of 570 nm.

2.7 Scanning Electron Microscopy

Mature biofilms and planktonic cells were fixed in 2.5% glutaraldehyde at 4 °C for 6 h. The cells were washed with PBS for four times. Then the specimens were dyed with 1% osmic acid solvent and subsequently washed with PBS for four times. Next, the samples were dehydrated by a gradient concentrations of ethanol (50%, 70%, 90% and 100%) for 10 min at each step. Finally, the dehydrated specimens were completely dried and analyzed using scanning electron microscopy (SEM) (TESCAN-MAIA3).

2.8 Transmission Electron Microscopy

Mature biofilms and planktonic cells were the first to be fixed with 2.5% glutaraldehyde at 4 °C for 6 h. The bacterial cells were washed with PBS for four times; the specimens were dyed with 1% osmic acid solvent and washed with PBS for four times. Then, the samples were dehydrated by a gradient concentrations of ethanol (50%, 70% and 90%), 90% ethanol: 90% propanone = 1:1(V/V), and 90% and 100% propanone for 10 min, respectively. After that, the cells were fixed with resin with propanone and epoxy at the ratios of 1:1 and 1:2, respectively, and fixed in a drying oven at 60 °C for 48 h. Finally, all the specimens were dissected with an ultramicrotome (LEICA EM UC7) and then analyzed on a transmission electron microscopy (TEM) (Talos L120C G2).

2.9 Data Analysis and Visualization

The MS raw data harvested from the analytical samples were firstly processed with an in-house software Agilent Qualitative Analysis, which integrated the peak signals of targeted metabolites and generated a three-dimensional data matrix with the peak area of the metabolite, metabolite ID and sample ID. After the peak area for each metabolite was normalized to the CFU value of each sample, the processed data were uploaded onto MetaboAnalyst version 4.0 (https://www.metaboanalyst.ca/MetaboAnalyst/) [22–24], to implement partial least-square discriminant analysis (PLS-DA) and heatmap overview. Bar plots and all other statistics were generated using Microsoft Office (Excel 2013) and MetaboAnalyst version 4.0.

3 Results

3.1 Mn^{2+} Regulated Biofilm Formation in a Concentration-Dependent Manner

To decipher the phenotypic features of the biofilm formation regulated by Mn^{2+} in *E. coli*, structural imaging, violet staining and CFU assay were combined to investigate the structure and physiological features of biofilm with the exposure to different concentrations of Mn^{2+}. Expectedly, our data indeed showed that Mn^{2+} can regulate biofilm formation, and the phenotypic changes were observed to render an obvious concentration-dependency of Mn^{2+}, and biofilm totally vanished when the addition of Mn^{2+} was up to 1000-fold of the original medium (Fig. 2). Since notable structural changes of biofilm and planktonic cells under different conditions were demonstrated in our preprint publication [8], thus, structural imaging method was also employed to confirm of how Mn^{2+} regulates the microstructure of biofilm and planktonic population. As we expected, the TEM and SEM images completely revealed that the fiber-layer, the EPS component, of biofilms treated with the defined concentration of Mn^{2+} (1000-fold), was remarkably eliminated compared to the original culture medium, which likely tends to the structure of planktonic cells (Fig. 3). This result was similar to that of our previous studies under different hypotheses and revealed that Mn^{2+} indeed regulates biofilm formation characterized by

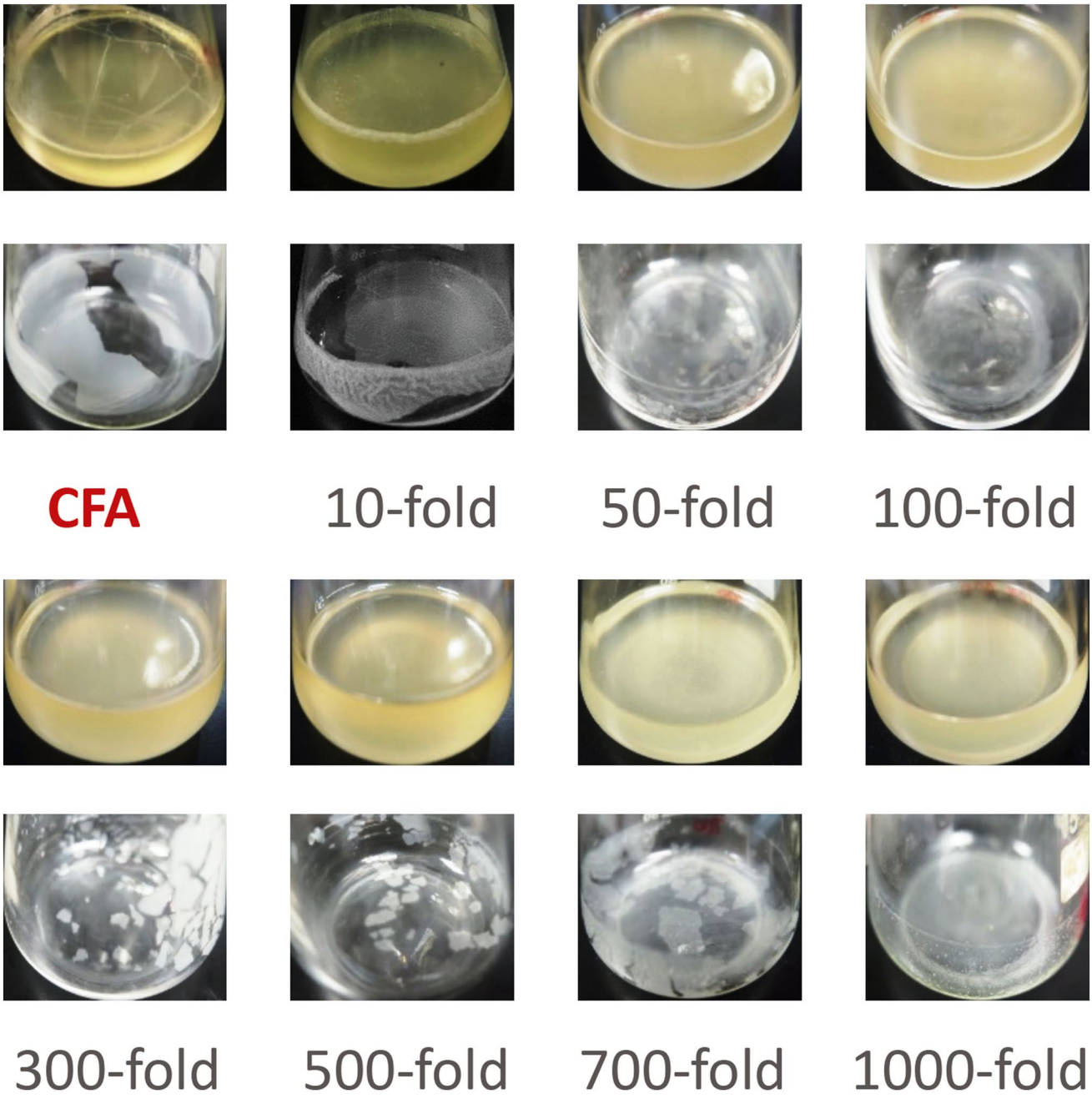

Fig. 2 Phenotypic imaging illustration of biofilm treated with different concentrations of Mn^{2+}

the distinct modifications in the biofilm structure [7, 8]. In addition, the violet staining and CFU assay were utilized to quantitatively analyze the biofilm formation under various concentrations of Mn^{2+} and further verified that the formation ability of biofilms is significantly impacted by Mn^{2+} with a concentration-dependent manner (Fig. S1). These phenotypic features of biofilms regulated by Mn^{2+} might suggest that biofilm formation triggered metabolic reprogramming is supposed to be regulated by Mn^{2+}.

3.2 Distinctly Metabolic Modifications Regulated by Mn^{2+} were Observed in Biofilm Formation

To interrogate the metabolic impact of Mn^{2+}on biofilm formation regulated in *E. coli*, we analyzed whether metabolic reprogramming of biofilm formation was regulated by Mn^{2+} or not, via using we newly developed targeted metabolomics method [19, 21]. To collect the reliable metabolome data, we highly selected the metabolites

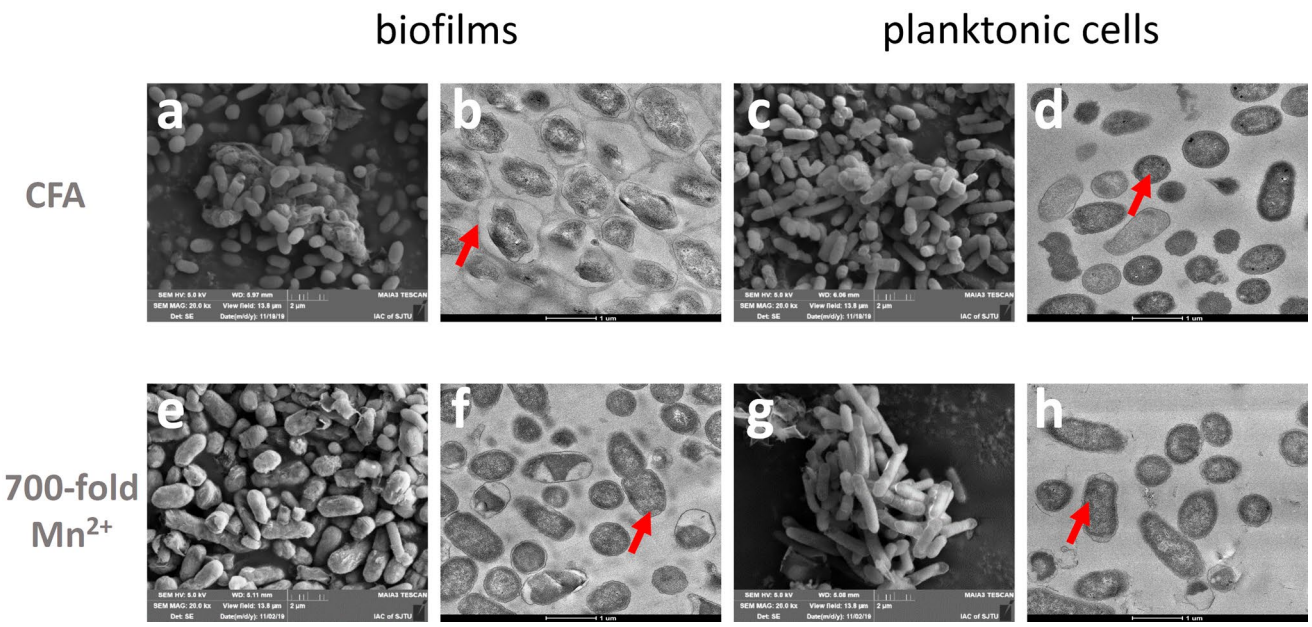

Fig. 3 Structural imaging illustration of biofilms and planktonic cells at pre- and post-treatment with 700-fold Mn^{2+} compared to the original culture medium. **a** SEM image of biofilms in original medium. **b** TEM image of biofilms in original medium. **c** SEM image of planktonic cells in original medium. **d** TEM image of planktonic cells in original medium. **e** SEM image of biofilms treated with 700-fold Mn^{2+} compared to the original culture medium. **f** TEM image of biofilms treated with 700-fold Mn^{2+} compared to the original culture medium. **g** SEM image of planktonic cells treated with 700-fold Mn^{2+} compared to the original culture medium. **h** TEM image of planktonic cells treated with 700-fold Mn^{2+} compared to the original culture medium

whose peak signals were quite high-quality and -reproducible for this study, to investigate how Mn^{2+} regulated small-molecule metabolism during biofilm formation (Table S2). The score plot resulted from PLS-DA analysis and heatmap-overview of metabolome data revealed that small-molecule metabolism of biofilms was significantly modified by the various concentration of Mn^{2+}, the modifications were dependent on the concentration of Mn^{2+} in the culture medium, whereas the metabolic pattern of biofilms under different concentrations of Mn^{2+} were obviously distinguished from the biofilms formed with original culture medium (Fig. 4). Collectively, 16 differential metabolites were discovered to phenotypically respond to the treatments of Mn^{2+} during biofilm formation (Table S3). These differential metabolites are glucose 6-phosphate, DL-glyceraldehyde 3-phosphate, pyridoxal 5′-phosphate (PLP), L-carnitine, L-lysine, citrate, isocitric acid, 5′-deoxy-5′-methylthioadenosine (5′-MTA), putrescine, tryptamine, serotonin, indole-3-acetic acid (IAA), oxidized glutathione, *N*-acetyl-glutamic acid, and glutaminate and aminobutyric acid (GABA). In short, our results confirmed that Mn^{2+} can modulate bacterial metabolism in a concentration-dependent manner, this might be a new biochemical mechanism of Mn^{2+} to regulate biofilm formation in microorganisms.

3.3 Important Metabolic Pathways were Characterized to be Regulated by Mn^{2+} During Biofilm Formation

To home the differential metabolites to their metabolic pathways, so that we could further elucidate the biochemical mechanism of these differential metabolites regulated by Mn^{2+} to impact biofilm formation, open-source database (KEGG) and related references were retrieved and summarized to reveal that small-molecule metabolisms involving glycolysis, TCA cycle and tryptophan metabolism were mostly regulated by Mn^{2+} during biofilm formation as most of the differential metabolites were homed to these pathways (Fig. 5). Therefore, annotation of biochemical functions implicated in these modified metabolic pathways can assist in elucidate the metabolic impact of Mn^{2+} on biofilm formation.

4 Discussion

It was reported that the activity changes of glycolysis play a role in biofilm formation, as proteomic analysis of biofilm-conditioned medium (BCM) and planktonic-conditioned medium (PCM) in *Staphylococcus aureus* showed

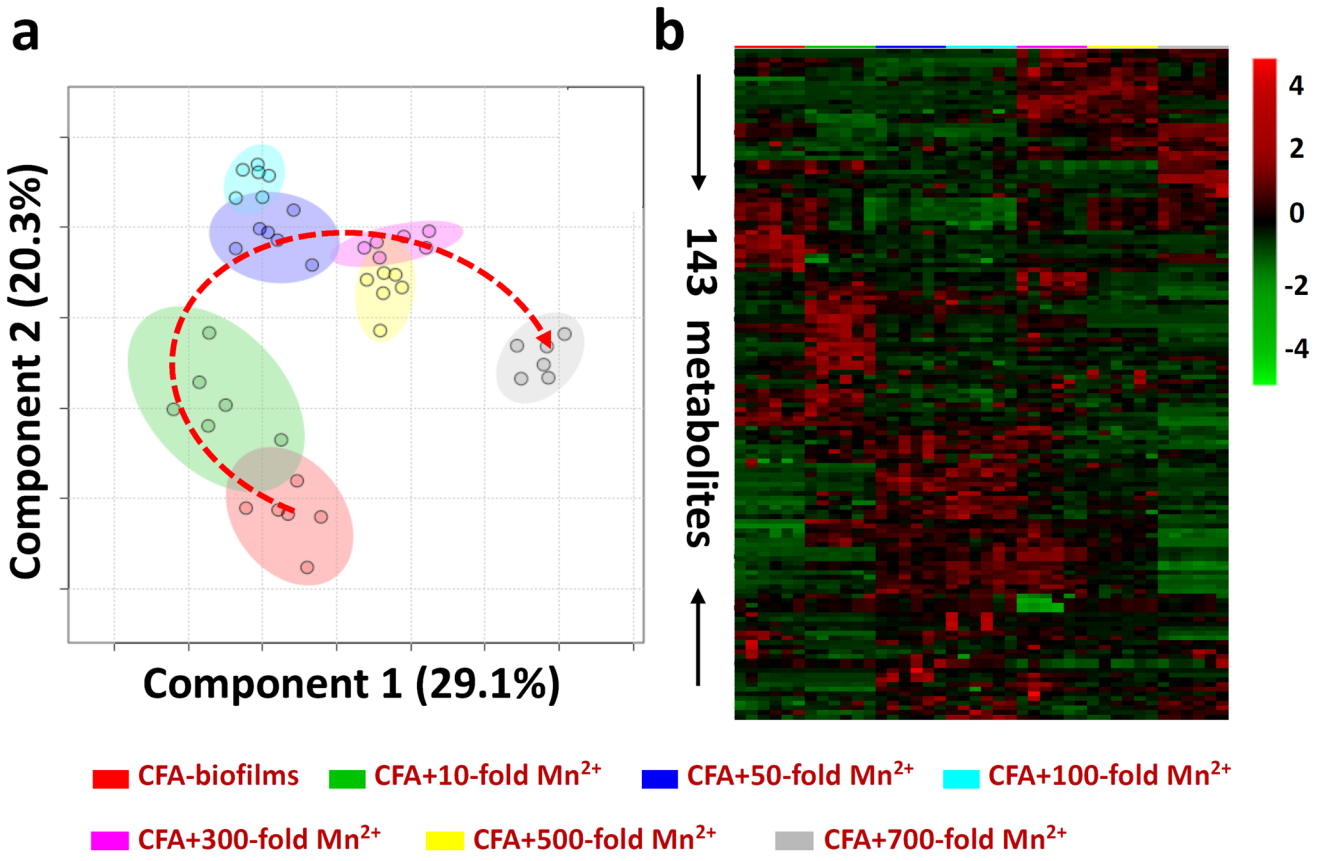

Fig. 4 Targeted-metabolomics analysis of biofilms treated with various concentrations of Mn^{2+}. **a** Score plot resulted from the supervised PLS-DA analysis of the selected metabolomes. **b** Heatmap-overview of the selected metabolomes

differential glycolytic enzymes were discovered, suggesting that central metabolic processes are significant difference in biofilms and planktonic cells; key metabolic enzyme with glycolysis glyceraldehyde-3-phosphate dehydrogenase was highly expressed in biofilm produced by *Staphylococcus xylosus*, and other studies also revealed the biochemical correlation between glycolysis and biofilm formation in *S. mutans* [25–27]. Interestingly, our data manifested glucose-6-phosphate, DL-glyceraldehyde 3-phosphate, and PLP, the main metabolites of glycolysis, were remarkably changed by Mn^{2+} control in biofilm formation induced by *E. coli* (Fig. 6a). In fact, glucose-6-phosphate isomerase was proved to be important in defense against oxidative stress in *Streptococcus equi ssp. zooepidemicus* [28]. Moreover, PdxR, homologous to the PLP-dependent aspartate aminotransferases, was found to regulate gene expression in biofilm formation in *S. mutans,* and PdxR-deficient mutant produced fewer biofilm [29]. YlmE, an ortholog of YggS, a highly conserved PLP-binding protein, was observed to involve in biofilm formation and disassembly in *E. coli* [30]. Mn^{2+} has been noticed to alter glycolysis by the regulation of the protein turnover and the reduction of energy production in *Solanum lycopersicum* [31], then microorganisms might employ metal-independent glycolytic isozymes to survive in a metal-limited environment [32, 33]. In short, metabolic reprogramming of glycolysis during biofilm formation in this study was confirmed again that Mn^{2+} regulates the activity of glycolysis to coordinate the energy production required for early stage of biofilm formation [28].

The TCA cycle is classified as a signal transduction pathway that could regulate biofilm formation and antibiotic susceptibility. Yet, biofilm formation was discovered to be initiated by several TCA cycle intermediates in a FnbA-dependent fashion in *S. aureus* [25, 34]. In our study, citrate, isocitric acid, L-carnitine, L-lysine, and 5′-MTA in the TCA cycle were mediated mostly by Mn^{2+} during biofilm formation (Fig. 6b). Sodium citrate was found to promote biofilm formation produced by *S. aureus* through inhibiting polysaccharide adhesin production and stimulating the interactions between cell and surface [34]. In addition, the biosynthesis of carnitine and carnitine-dependent transformation of acetyl-coA assist in biofilm formation in *Candida albicans* [35]. Palmitoyl-DL-carnitine has also been characterized as an inhibitor of *Pseudomonas aeruginosa* and *E. coli* biofilm development via affecting multiple metabolic pathways, motility, and second messenger [36]. What's more, the previous study discovered that 5′-MTA alters

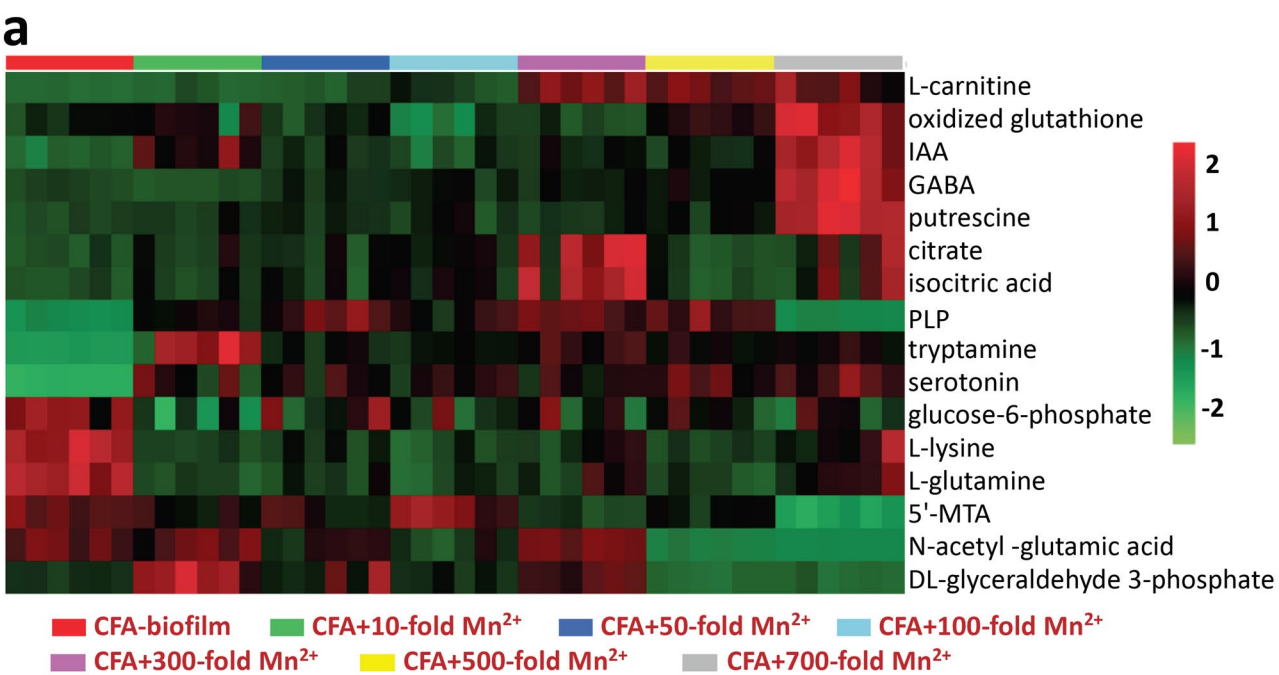
a
L-carnitine
oxidized glutathione
IAA
GABA
putrescine
citrate
isocitric acid
PLP
tryptamine
serotonin
glucose-6-phosphate
L-lysine
L-glutamine
5'-MTA
N-acetyl -glutamic acid
DL-glyceraldehyde 3-phosphate
2
1
0
-1
-2
CFA-biofilm
CFA+10-fold Mn2+
CFA+50-fold Mn2+
CFA+100-fold Mn2+
CFA+300-fold Mn2+
CFA+500-fold Mn2+
CFA+700-fold Mn2+

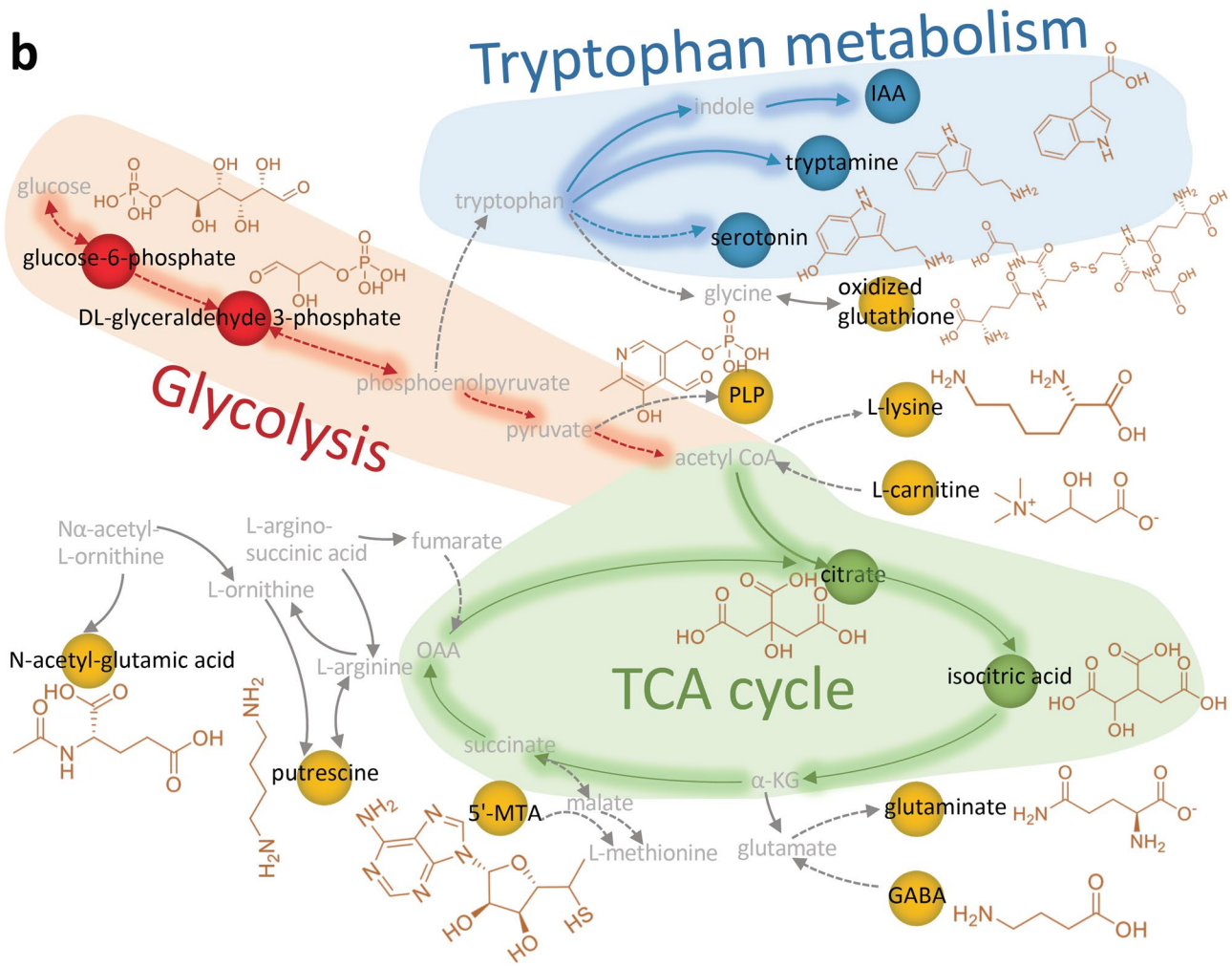
b
Tryptophan metabolism
indole
IAA
tryptamine
tryptophan
serotonin
glycine
oxidized glutathione
glucose
glucose-6-phosphate
DL-glyceraldehyde 3-phosphate
Glycolysis
phosphoenolpyruvate
pyruvate
PLP
L-lysine
acetyl CoA
L-carnitine
Nα-acetyl-L-ornithine
L-argino-succinic acid
fumarate
L-ornithine
citrate
N-acetyl-glutamic acid
L-arginine
OAA
TCA cycle
isocitric acid
succinate
α-KG
putrescine
5'-MTA
malate
L-methionine
glutaminate
glutamate
GABA

◂**Fig. 5** Functional metabolites and associated metabolic pathways were mostly regulated by Mn^{2+} during biofilm formation. **a** Heatmap overview of the identified functional metabolites. **b** The mostly affected metabolic pathways

the quorum sensing (QS) signal system, and further modulates biofilm formation and virulence in several strains [8]. Moreover, Mn^{2+} has also been observed to change energy metabolism by modulating the activities of various glycolytic and TCA cycle enzymes in neural cells [37]. Our finding might indicate that Mn^{2+} could also interfere TCA cycle and further mediate signal transduction to regulate biofilm formation in *E. coli*.

In addition, indole metabolism has been investigated to affect biofilm formation but the regulations are unagreeable among different microorganisms [38–41]. There is increasing evidence to manifest that tryptophan can inhibit biofilm formation in several microorganisms, such as *P. aeruginosa*, *Cronobacter sakazakii,* and *E. coli* through catalyzing into indole and suppressing QS system [42–45]. In our results, IAA, serotonin, tryptamine, and oxidized glutathione which are closely associated with tryptophan metabolism, can be regulated by Mn^{2+} during biofilm formation (Fig. 6c). It has been demonstrated that IAA could promote biofilm formation in *iacA* mutants but not the wild type of *Acinetobacter baumannii* via enhancing the expression of IAA-degradative genes [46]; silver-indole-3-acetic acid hydrazide (IAAH – Ag) complexes were verified to efficiently inhibit multidrug-resistant clinical isolates in biofilms in several organisms [47]. Moreover, 5-HT, a kind of gun serotonin, was found to induce the adhesion and invasion of commensal *E. coli*, but not to affect biofilm formation [48]. Intracellular glutathione level was found to be regulated by manganese, which was agreeable with our discovery [49]. At last, GABA could regulate the lipopolysaccharide (LPS) structure and cytotoxicity, which is specific to some strains, for example, *Pseudomonas fluorescens* [50], and GABA only affected the early phases of bacterial adhesion [51], which might account for our discovery as Mn^{2+} regulate GABA to yield impact on biofilm formation.

In short, our finding revealed that Mn^{2+} could inhibit biofilm formation through the regulation of glycolysis, TCA cycle, and tryptophan metabolism. Next, we shall figure out to elucidate the biochemical mechanism of how Mn^{2+} regulates these functional metabolites and associated metabolic pathways to further intervene biofilm formation in different microorganisms.

5 Conclusion

To investigate the metabolic impact of Mn^{2+} on biofilm formation in *Escherichia coli,* we were the first to characterize small-molecule metabolism regulated by Mn^{2+} during biofilm formation, using targeted metabolomics method, combined with structural imaging assay. Our data demonstrated that Mn^{2+} can mediate biofilm formation in a concentration-dependent manner, then we further precisely characterized 16 functional metabolites and associated 3 metabolic pathways involving glycolysis, TCA cycle, and tryptophan metabolism were mostly changed by Mn^{2+} that underlie in the biochemical regulation of biofilm formation. Collectively, our finding provides novel insight into the impact of Mn^{2+} on biofilm formation from a metabolic perspective, thus, allowing to design and develop novel strategies to eradicate biofilm formation in different microorganisms by targeting the regulation of Mn^{2+} to biosynthesis and expressions of functional metabolites, by which we can address the challenging issues related to biofilm formation in different niches.

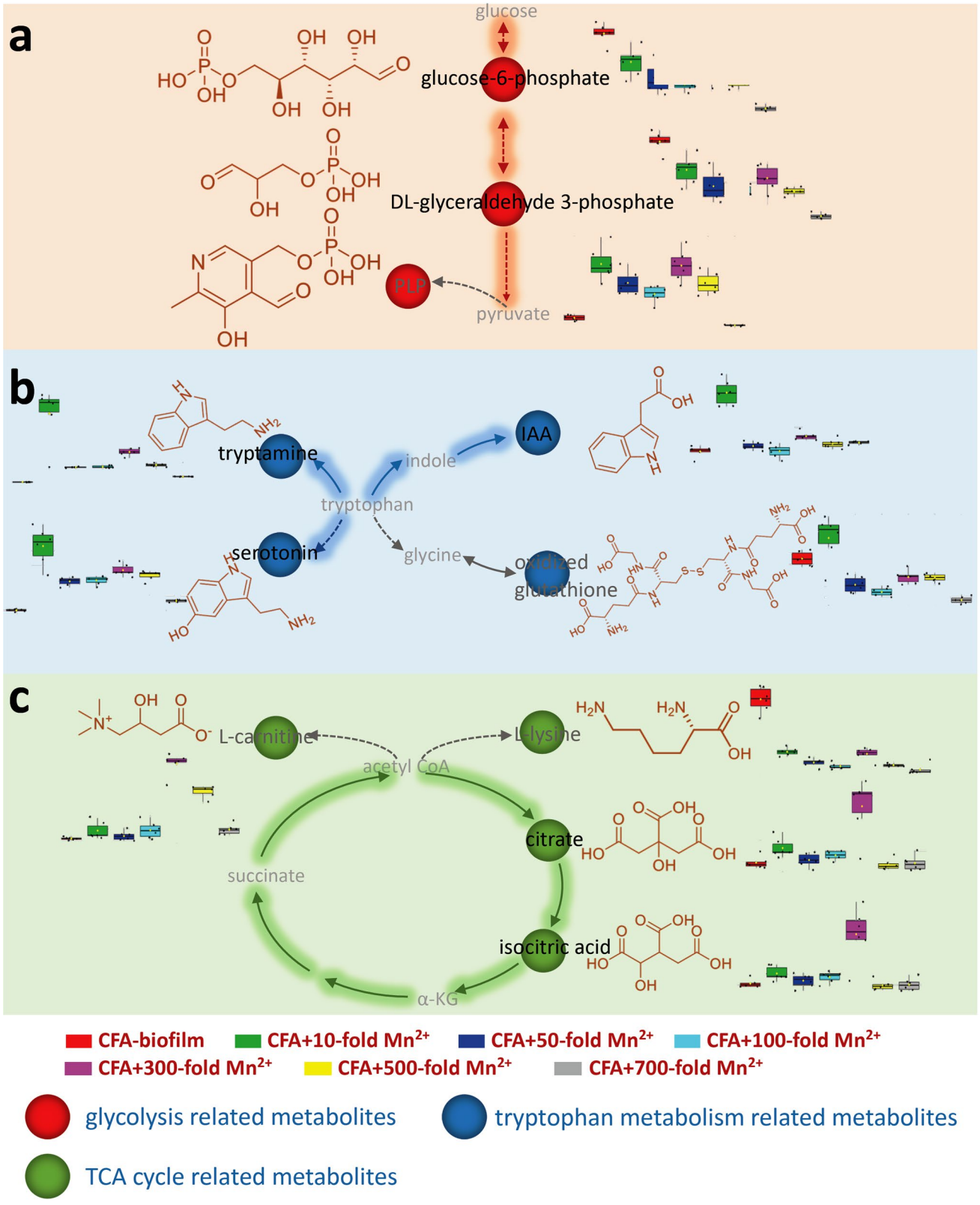

Fig. 6 Qualitative and quantitative characterization of the functional metabolites and associated metabolic pathways, whose level changes respond to different concentrations of Mn^{2+}. **a** Glycolysis and related functional metabolites. **b** TCA cycle and related functional metabolites. **c** Tryptophan metabolism and related functional metabolites

Acknowledgements This work was supported by the National Key R&D Program of China (No. 2017YFC1308600 and 2017YFC1308605), the National Natural Science Foundation of China Grants (No. 31670031), the Startup Funding for Specialized Professorship Provided by Shanghai Jiao Tong University (No. WF220441502).

Author contributions HL conceived and designed the study; RG performed the study and collected the data; RG and HL analyzed and interpreted the data; RG and HL wrote the manuscript.

Compliance with ethical standards

Conflict of interest All authors declare that they have no conflicts of interest.

References

1. Luo X, Guo R, Xu X, Li X, Yao L, Wang X, Lu H. Mass spectrometry and associated technologies delineate the advantageously biomedical capacity of siderophores in different pathogenic contexts. Mass Spectrom Rev. 2019;38(3):239–52.
2. Guilhen C, Miquel S, Charbonnel N, Joseph L, Carrier G, Forestier C, Balestrino D. Colonization and immune modulation properties of Klebsiella pneumoniae biofilm-dispersed cells. Npj Biofilms Microb. 2019;5(1):1–11.
3. Penesyan A, Nagy SS, Kjelleberg S, Gillings MR, Paulsen IT. Rapid microevolution of biofilm cells in response to antibiotics. Npj Biofilms Microb. 2019;5(1):1–14.
4. Mukherjee M, Hu Y, Tan CH, Rice SA, Cao B. Engineering a light-responsive, quorum quenching biofilm to mitigate biofouling on water purification membranes. Sci Adv. 2018;4(12):u1459.
5. Bowen WH, Burne RA, Wu H, Koo H. Oral biofilms: pathogens, matrix, and polymicrobial interactions in microenvironments. Trends Microbiol. 2018;26(3):229–42.
6. Ma W, Peng D, Walker SL, Cao B, Gao C, Huang Q, Cai P. Bacillus subtilis biofilm development in the presence of soil clay minerals and iron oxides. Npj Biofilms Microb. 2017;3(1):4–9.
7. Lu H, Que Y, Wu X, Guan T, Guo H. Metabolomics deciphered metabolic reprogramming required for biofilm formation. Sci Rep-Uk. 2019;9(1):13160.
8. Guo R, Luo X, Liu J, Lu H. Novel functional metabolites that affect biofilm formation are regulated by bioavailable iron with siderophore-dependent pathway. bioRxiv. 2020. https://doi.org/10.1101/2020.03.04.977660.
9. Shafeeq S, Pannanusorn S, Elsharabasy Y, Ramírez-Zavala B, Morschhäuser J, Römling U. Impact of manganese on biofilm formation and cell morphology of *Candida parapsilosis* clinical isolates with different biofilm forming abilities. Fems Yeast Res. 2019;19(6):057.
10. Richard H, Carpenter EJ, Komada T, Palmer PT, Rochman CM. Biofilm facilitates metal accumulation onto microplastics in estuarine waters. Sci Total Environ. 2019;683:600–8.
11. Krishnan M, Dahms HU, Seeni P, Gopalan S, Sivanandham V, Jin-Hyoung K, James RA. Multi metal assessment on biofilm formation in offshore environment. Mater Sci Eng C Mater Biol Appl. 2017;73:743–55.
12. Abinaya SP, Gautam P. Studies on the biofilm produced by *Pseudomonas aeruginosa* grown in different metal fatty acid salt media and its application in biodegradation of fatty acids and bioremediation of heavy metal ions. Can J Microbiol. 2017;63(1):61–73.
13. Mhatre E, Troszok A, Gallegos-Monterrosa R, Lindstädt S, Hölscher T, Kuipers OP, Kovács ÁT. The impact of manganese on biofilm development of *Bacillus subtilis*. Microbiology. 2016;162(8):1468–78.
14. Arirachakaran P, Luengpailin S, Banas JA, Mazurkiewicz JE, Benjavongkulchai E. Effects of manganese on *Streptococcus mutans* planktonic and biofilm growth. Caries Res. 2007;41(6):497–502.
15. Sihra N, Goodman A, Zakri R, Sahai A, Malde S. Nonantibiotic prevention and management of recurrent urinary tract infection. Nature reviews. Urology. 2018;15(12):750–76.
16. Halouane F, Jijie R, Meziane D, Li C, Singh SK, Bouckaert J, Jurazek J, Kurungot S, Barras A, Li M, Boukherroub R, Szunerits S. Selective isolation and eradication of *E. coli* associated with urinary tract infections using anti-fimbrial modified magnetic reduced graphene oxide nanoheaters. J Mater Chem B. 2017;5(40):8133–42.
17. Spaulding CN, Klein RD, Ruer S, Kau AL, Schreiber HL, Cusumano ZT, Dodson KW, Pinkner JS, Fremont DH, Janetka JW, Remaut H, Gordon JI, Hultgren SJ. Selective depletion of uropathogenic *E. coli* from the gut by a FimH antagonist. Nature. 2017;546(7659):528–32.
18. Hung C, Zhou Y, Pinkner JS, Dodson KW, Crowley JR, Heuser J, Chapman MR, Hadjifrangiskou M, Henderson JP, Hultgren SJ. *Escherichia col*i biofilms have an organized and complex extracellular matrix structure. Mbio. 2013;4(5):e645.
19. Luo X, Zhang A, Wang X, Lu H. UHPLC/MS based large-scale targeted metabolomics method for multiple-biological matrix assay. bioRxiv. 2019. https://doi.org/10.1101/642496.
20. Lv H, Hung CS, Henderson JP. Metabolomic analysis of siderophore cheater mutants reveals metabolic costs of expression in uropathogenic *Escherichia coli*. J Proteome Res. 2014;13(3):1397–404.
21. Luo X, Liu J, Wang H, Lu H. Metabolomics identified new biomarkers for the precise diagnosis of pancreatic cancer and associated tissue metastasis. Pharmacol Res. 2020. https://doi.org/10.1016/j.phrs.2020.104805.
22. Chong J, Wishart DS, Xia J. Using MetaboAnalyst 4.0 for comprehensive and integrative metabolomics data analysis. Curr Protoc Bioinf. 2019;68(1).
23. Chong J, Yamamoto M, Xia J. MetaboAnalystR 2.0: from raw spectra to biological insights. Metabolites. 2019;9(3):57.
24. Chong J, Xia J. MetaboAnalystR: an R package for flexible and reproducible analysis of metabolomics data. Bioinformatics. 2018;34(24):4313–4.
25. Secor PR, James GA, Fleckman P, Olerud JE, McInnerney K, Stewart PS. *Staphylococcus aureus* biofilm and planktonic cultures differentially impact gene expression, mapk phosphorylation, and cytokine production in human keratinocytes. Bmc Microbiol. 2011;11:143.
26. Planchon S, Desvaux M, Chafsey I, Chambon C, Leroy S, Hébraud M, Talon R. Comparative subproteome analyses of planktonic and sessile *Staphylococcus xylosus* C2a: new insight in cell physiology of a coagulase-negative Staphylococcus in Biofilm. J Proteome Res. 2009;8(4):1797–809.
27. Rathsam C, Eaton RE, Simpson CL, Browne GV, Berg T, Harty DWS, Jacques NA. Up-regulation of competence-but not stress-responsive proteins accompanies an altered metabolic phenotype in Streptococcus mutans biofilms. Microbiology+. 2005;151(6):1823–37.
28. Yi L, Wang Y, Ma Z, Zhang H, Li Y, Zheng J, Yang Y, Fan H, Lu C. Biofilm formation of Streptococcus equi ssp. zooepidemicus and comparative proteomic analysis of biofilm and planktonic cells. Curr Microbiol. 2014;69(3):227–33.
29. Liao S, Bitoun JP, Nguyen AH, Bozner D, Yao X, Wen ZT. Deficiency of PdxR in Streptococcus mutans affects vitamin B6 metabolism, acid tolerance response and biofilm formation. Mol Oral Microbiol. 2015;30(4):255–68.

30. Ito T, Yamauchi A, Hemmi H, Yoshimura T. Ophthalmic acid accumulation in an *Escherichia coli* mutant lacking the conserved pyridoxal 5'-phosphate-binding protein YggS. J Biosci Bioeng. 2016;122(6):689–93.
31. Ceballos-Laita L, Gutierrez-Carbonell E, Imai H, Abadía A, Uemura M, Abadía J, López-Millán AF. Effects of manganese toxicity on the protein profile of tomato (*Solanum lycopersicum*) roots as revealed by two complementary proteomic approaches, two-dimensional electrophoresis and shotgun analysis. J Proteomics. 2018;185:51–63.
32. Radin JN, Kelliher JL, Solórzano PKP, Grim KP, Ramezanifard R, Slauch JM, Kehl-Fie TE. Metal-independent variants of phosphoglycerate mutase promote resistance to nutritional immunity and retention of glycolysis during infection. Plos Pathog. 2019;15(7):e1007971.
33. Párraga Solórzano PK, Yao J, Rock CO, Kehl-Fie TE. Disruption of glycolysis by nutritional immunity activates a two-component system that coordinates a metabolic and antihost response by *Staphylococcus aureus*. Mbio. 2019;10(4):e1319–e13211321.
34. Robert MQS, Meehl MA, Brothers KM, Martinez RM, Donegan NP, Graber ML, Cheung AL, O'Toole GA. Genetic evidence for an alternative citrate-dependent biofilm formation pathway in *Staphylococcus aureus* that is dependent on fibronectin binding proteins and the GraRS two-component regulatory system. Infect Immun. 2008;76(6):2469–77.
35. Nieminen MT, Novak-Frazer L, Rautemaa V, Rajendran R, Sorsa T, Ramage G, Bowyer P, Rautemaa R. A novel antifungal is active against *Candida albicans* biofilms and inhibits mutagenic acetaldehyde production in vitro. PLoS ONE. 2014;9(5):e97864.
36. Wenderska IB, Chong M, McNulty J, Wright GD, Burrows LL. Palmitoyl-dl-carnitine is a multitarget inhibitor of *Pseudomonas aeruginosa* biofilm development. ChemBioChem. 2011;12(18):2759–66.
37. Malthankar GV, White BK, Bhushan A, Daniels CK, Rodnick KJ, Lai JCK. Differential lowering by manganese treatment of activities of glycolytic and tricarboxylic acid (TCA) cycle enzymes investigated in neuroblastoma and astrocytoma cells is associated with manganese-induced cell death. Neurochem Res. 2004;29(4):709–17.
38. Lee J, Jayaraman A, Wood TK. Indole is an inter-species biofilm signal mediated by SdiA. Bmc Microbiol. 2007;7(1):42.
39. Hu M, Zhang C, Mu Y, Shen Q, Feng Y. Indole affects biofilm formation in bacteria. Indian J Microbiol. 2010;50(4):362–8.
40. Konopelski P, Ufnal M. Indoles—gut bacteria metabolites of tryptophan with pharmacotherapeutic potential. Curr Drug Metab. 2018;19(10):883.
41. Pandey R, Swamy KV, Khetmalas MB. Indole: a novel signaling molecule and its applications. Indian J Biotechnol. 2013;12:297–310.
42. Brandenburg KS, Rodriguez KJ, McAnulty JF, Murphy CJ, Abbott NL, Schurr MJ, Czuprynski CJ. Tryptophan inhibits biofilm formation by *Pseudomonas aeruginosa*. Antimicrob Agents Chemother. 2013;57(4):1921–5.
43. Shimazaki J, Furukawa S, Ogihara H, Morinaga Y. L-tryptophan prevents *Escherichia coli* biofilm formation and triggers biofilm degradation. Biochem Bioph Res Commun. 2012;419(4):715–8.
44. Li H, Ye Y, Ling N, Wu Q, Zhang J. Inhibitory effects of D-tryptophan on biofilm development by the foodborne *Cronobacter sakazakii*. Int Dairy J. 2015;49:125–9.
45. Chakraborty P, Daware AV, Kumari M, Chatterjee A, Bhattacharyya D, Mitra G, Akhter Y, Bhattacharjee S, Tribedi P. Free tryptophan residues inhibit quorum sensing of *Pseudomonas aeruginosa*: a potential approach to inhibit the development of microbial biofilm. Arch Microbiol. 2018;200(10):1419–25.
46. Lin H, Shu H, Lin G. Biological roles of indole-3-acetic acid in *Acinetobacter baumannii*. Microbiol Res. 2018;216:30–9.
47. Kuthati Y, Kankala RK, Lin S, Weng C, Lee C. pH-Triggered controllable release of silver–indole-3 acetic acid complexes from mesoporous silica nanoparticles (IBN-4) for effectively killing malignant bacteria. Mol Pharmaceut. 2015;12(7):2289–304.
48. Banskota S, Regmi SC, Gautam J, Gurung P, Lee Y, Ku SK, Lee J, Lee J, Chang HW, Park SJ, Kim J. Serotonin disturbs colon epithelial tolerance of commensal *E. coli* by increasing NOX2-derived superoxide. Free Radical Bio Med. 2017;106:196–207.
49. Dittman EK, Buchwalter DB. Manganese bioconcentration in aquatic insects: Mn oxide coatings, molting loss, and Mn(II) thiol scavenging. Environ Sci Technol. 2010;44(23):9182–8.
50. Dagorn A, Chapalain A, Mijouin L, Hillion M, Duclairoir-Poc C, Chevalier S, Taupin L, Orange N, Feuilloley M. Effect of GABA, a bacterial metabolite, on *Pseudomonas fluorescens* surface properties and cytotoxicity. Int J Mol Sci. 2013;14(6):12186–204.
51. Dagorn A, Hillion M, Chapalain A, Lesouhaitier O, Duclairoir Poc C, Vieillard J, Chevalier S, Taupin L, Le Derf F, Feuilloley MGJ. Gamma-aminobutyric acid acts as a specific virulence regulator in *Pseudomonas aeruginosa*. Microbiology. 2013;159(Pt2):339–51.